The glass transition and diffusion in simulated liquid TiO_2

2007 J. Phys.: Condens. Matter 19 416109

(http://iopscience.iop.org/0953-8984/19/41/416109)

IOP PUBLISHING JOURNAL OF PHYSICS: CONDENSED MATTER

J. Phys.: Condens. Matter **19** (2007) 416109 (13pp) doi:10.1088/0953-8984/19/41/416109

The glass transition and diffusion in simulated liquid TiO_2

Vo Van Hoang

Department of Physics, Institute of Technology, National University of HochiMinh City, 268 Ly Thuong Kiet Street, District 10, HochiMinh City, Vietnam

E-mail: vvhoang2002@yahoo.com

Received 15 August 2007
Published 27 September 2007
Online at stacks.iop.org/JPhysCM/19/416109

Abstract

The glass transition and diffusion in liquid TiO_2 have been studied in a model containing 3000 atoms via molecular dynamics (MD) simulation. The density dependence of the glass transition temperature, T_g, of liquid TiO_2 has been found and is discussed. Diffusion of atomic species in 3.80 g cm^{-3} TiO_2 models has been investigated over a wide temperature range from 2100 to 7000 K. We found that the temperature dependence of the diffusion constant of atomic species follows an Arrhenius law at relatively low temperatures above the melting point, and at higher temperatures it deviates from an Arrhenius law. Differences between the structures of amorphous TiO_2 models at three different densities in the range from 3.80 to 4.20 g cm^{-3} have been found and are discussed. In addition, a transition from a low-density liquid (ldl) form to a high-density liquid (hdl) form was found and is discussed.

1. Introduction

For the past three decades, much attention has been given to TiO_2 and titanium oxide-based materials due to their useful photocatalytic, optical, thermal and mechanical properties (see [1–18] and references therein). Titanium oxide naturally occurs in the three polymorphs: rutile, anatase and brookite; of them, rutile is the most common in nature and the most stable phase under ambient conditions [3]. On the other hand, for technological reasons TiO_2 is mainly produced as thin film, powder or nanoparticles by employing various techniques such as electron or ion beam deposition, reactive evaporation, plasma plating, sputtering or the relatively new sol–gel method, etc [4, 6, 9, 11, 12, 14, 17]. The initially obtained titania is usually amorphous or poorly crystalline, and it is further thermally treated in order to get materials with the desired technological properties. It has been found that thermal treatment affects both the morphology and the atomic-scale structure of the initially produced TiO_2. Depending on the sample technological history, phase transitions from amorphous to different crystalline states such as anatase [18–20], rutile [21] or brookite [22] might occur upon further

thermal treatment. This means that amorphous TiO_2 is an important phase among TiO_2 polymorphs. On the other hand, this material also has an importance in both technology and materials science due to its short-range order structure that is different from its crystalline counterparts. Indeed, much attention has been paid to the structure, properties and different applications of amorphous TiO_2 by both experiments and computer simulations (see [9] and references therein). So far, our understanding of the structure and properties of amorphous TiO_2 is poor, and detailed information on an atomistic level can be provided by computer simulation. There is a limited number of simulation works related to the liquid and amorphous TiO_2; this may be due to the lack of good interatomic potentials for the system. Petkov *et al* used reverse Monte Carlo simulations to highlight the microscopic structure of amorphous TiO_2 together with an experimental analysis, and the atomic arrangement in amorphous TiO_2 has been found to resemble that which occurs in brookite and is an assembly of short, staggered chains of TiO_6 octahedra [9]. Our recent MD simulation results of liquid and amorphous TiO_2 at the density of 3.80 g cm^{-3} share many trends observed by Petkov *et al*, and the local structure of amorphous TiO_2 has been analyzed in more detail [23].

However, our understanding of the structure and properties of liquid and amorphous TiO_2 is still limited. No work related to the diffusion of atomic species in liquid TiO_2, the glass transition or the density dependence of the local structure of amorphous TiO_2 has been found in the literature. Therefore, it is worth carrying out such a study by computer simulation, and this is our main aim here in the present work.

2. Calculations

We carry out the simulations for liquid and amorphous TiO_2 models in a cube under periodic boundary conditions containing 3000 atoms (both Ti and O atoms together). We use the Verlet algorithm, and one MD step is equal to 1.6 fs. Several interatomic potentials have been reported for crystalline TiO_2 (see [3, 24–33]). Through a detailed analysis of the different force fields for titania, Collins *et al* concluded that the force field developed for crystalline TiO_2 proposed by Matsui and Akaogi (MA) is the most suitable for MD simulating TiO_2 (see [3, 33]). The MA potentials are composed of the pairwise additive Coulomb, dispersion and repulsion interactions. The energy parameters of the MA potentials were determined to reproduce the crystal structures of rutile, anatase and brookite, and the measured elastic constants of rutile. By using such potentials they successfully reproduced a wide range of properties of the four polymorphs of TiO_2 crystals mentioned above, including the crystal structures, volume compressibility, volume thermal expansivity and enthalpy relationships between them. After intensive testing we found that the MA potentials are good for simulating liquid and amorphous TiO_2 [23]. The MA potentials have the following form [3]:

$$U_{ij}(r) = Z_i Z_j \frac{e^2}{r} + f(B_i + B_j)\exp[(A_i + A_j - r)/(B_i + B_j)] - \frac{C_i C_j}{r^6}, \tag{1}$$

with i, j = Ti, O. Here r is the interatomic distance and Z_i, Z_j are the charges of ions: $Z_{Ti} = +2.196$ and $Z_O = -1.098$. The quantity f is a standard force of 4.184 kJ $Å^{-1}$ mol^{-1}. The other parameters of the potentials are shown in table 1. More details about the MA potentials can be found in [3].

Coulomb interactions were taken into account by means of the Ewald–Hansen method [34]. The equilibrated melt at 7000 K was obtained by relaxing a random configuration over 5×10^4 MD steps. The system was cooled down from the melt at constant volume corresponding to the adopted density. The temperature of the system was controlled by the velocity scaling. The temperature of the system was decreased linearly in time as $T = T_0 - \gamma t$;

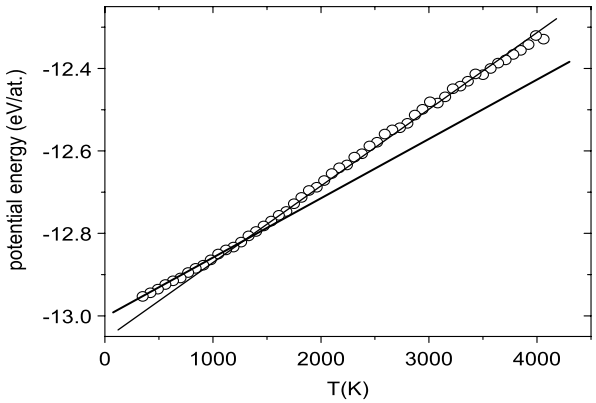

Figure 1. Temperature dependence of the potential energy of the 3.80 g cm^{-3} TiO_2 model.

Table 1. Energy parameters of the MA potentials.

Element	A (Å)	B (Å)	C (Å^3 kJ$^{\frac{1}{2}}$ mol$^{-\frac{1}{2}}$)
Ti	1.1823	0.077	22.5
O	1.6339	0.117	54.0

here γ is a cooling rate of 4.2945×10^{13} K s^{-1} and T_0 is the initial temperature of 7000 K. Because the density of amorphous TiO_2 is not unique (it depends on the purity of the samples), we paid great attention to the value of 3.80 g cm^{-3}, which is close to that obtained in practice for amorphous TiO_2 films [35]. However, the density of crystalline TiO_2 is 3.83 g cm^{-3}, 4.17 g cm^{-3} and 4.24 g cm^{-3} for anatase, brookite and rutile, respectively [12]. Therefore, we also simulated amorphous TiO_2 models at three different densities, 3.80, 4.00 and 4.20 g cm^{-3}, in order to compare the structures with each other. The glass transition temperature was determined in models at five different densities ranging from 3.80 to 5.00 g cm^{-3} in order to observe the density dependence of T_g. In order to calculate the coordination number distributions and bond-angle distributions in liquid and amorphous TiO_2, we adopted the fixed values $R_{Ti-Ti} = 4.00$ Å, $R_{Ti-O} = 2.50$ Å and $R_{O-O} = 3.50$ Å. Here R denotes a cutoff radius, which was chosen as the position of the minimum after the first peak in the partial radial distribution function (PRDF) for the amorphous state at 350 K and at 3.80 g cm^{-3}. The amorphous models at 350 K were relaxed over 5×10^4 MD steps before evaluating the static quantities. In order to improve the statistics of the results for diffusion of atomic species in liquid TiO_2 at 3.80 g cm^{-3}, calculated data for diffusion were averaged over two independent runs and the system at each temperature was relaxed over 10^5 MD steps (or 160 ps).

3. Results and discussion

3.1. Density dependence of the glass transition temperature T_g

The glass phase transition temperature, T_g, is an important quantity of glasses, and its determination attracts great interest. We determined T_g via the intersection of a linear high- and low-temperature extrapolation of the system potential energy as was done for GeO_2 [36]. As shown in figure 1, T_g of liquid TiO_2 at 3.80 g cm^{-3} is equal to 1250 K. There is no experimental value for T_g of liquid TiO_2 to compare with. However, this value is not far

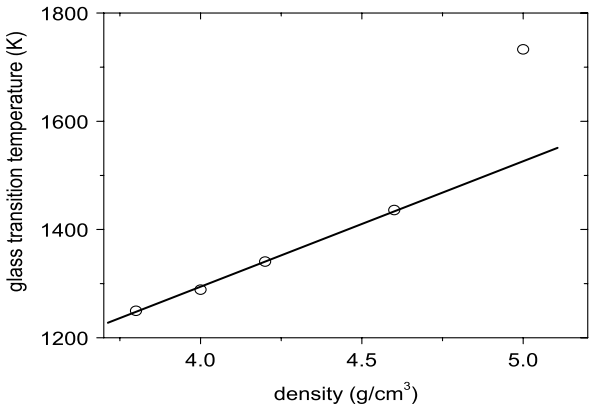

Figure 2. Density dependence of the glass transition temperature of liquid TiO_2 models.

from the value $T_g = 1450$ K for silica obtained in practice [36]. It is essential to notice that the melting temperature for crystalline TiO_2 is $T_m = 2123$ K [37]. On the other hand, due to the unrealistic high quenching rates used in the simulation (i.e. around 10^{12}–10^{13} K s^{-1} versus the experimental value of around 10^6–10^7 K s^{-1}), a discrepancy between simulated and experimental T_g can be expected. In order to highlight the cooling rate effects on T_g of liquid TiO_2 at 3.80 g cm^{-3}, we estimated T_g by using three different cooling rates. We found that T_g is equal to 1465 and 1217 K for the cooling rates of 4.2945×10^{14} and 8.589×10^{12} K s^{-1}, respectively. This means that T_g decreases with decreasing cooling rate like those usually found in practice or by computer simulation. Basing on the power of current computers one cannot apply cooling rates of around 10^6–10^7 K s^{-1} like those used in practice. And hence, via extrapolating to the lower cooling rates often used in practice, we found $T_g \approx 1200$ K for liquid TiO_2 at the ambient pressure density. Moreover, the density of amorphous TiO_2 is not unique; it depends on the fabricating conditions and on the content of impurity in the samples [35]. Therefore, it is worth studying the density dependence of T_g for liquid TiO_2. We also found the value for T_g of liquid TiO_2 at different densities via the temperature dependence of the system potential energy. We found that T_g is equal to 1250, 1289, 1341, 1436 and 1733 K for the system at 3.80, 4.00, 4.20, 4.60 and 5.00 g cm^{-3}, respectively. Figure 2 shows that T_g increases linearly with the density. However, at the very high density of 5.00 g cm^{-3}, a strong deviation from linearity was found. Possibly, at relatively low densities the linear enhancement of T_g is caused by the close-packing structure effects. At the very high density of 5.00 g cm^{-3}, an ldl $\rightarrow$ hdl transition might occur in the system, and this would lead to the strong deviation from linearity of the curve presented in figure 2. It is essential to notice that the high-density amorphous form of TiO_2 has been found at high pressure in practice and it is worth carrying out a study in this direction [38].

We found the linear density dependence of T_g for liquid TiO_2 over densities ranging from 3.80 to 4.60 g cm^{-3} to be $T_g = a + b\rho$. Here, $a = 352$ K, $b = 235.43$ cm^3 g^{-1} and ρ is the density of liquid TiO_2 in g cm^{-3}. The pressure dependence (or density dependence) of the glass transition temperature attracts great interest; however, due to the difficulty in carrying out experiments at very high pressures there is a limited number of works related to the pressure dependence of T_g. For example, the effect of pressure on the glass transition temperature T_g has been estimated via the temperature dependence of the DC electric conductivity in alkaline, alkaline earth silicate and silica glasses [39]. According to the data presented in [39], T_g increases or decreases linearly with pressure P depending on the substances. The

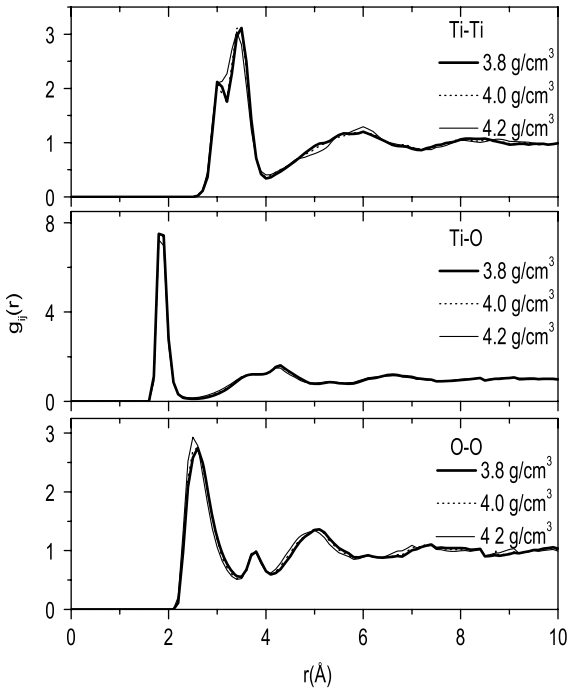

Figure 3. Radial distribution functions of amorphous TiO_2 models at $T = 350$ K.

value of T_g in anorthite glass varies with pressure as $T_g = 848\,^{\circ}\text{C} + 5.3\,^{\circ}\text{C GPa}^{-1} \times P$ (pressure P in GPa), in albite as $T_g = 688\,^{\circ}\text{C} - 9.4\,^{\circ}\text{C GPa}^{-1} \times P$ and in silica glass as $T_g = 1050\,^{\circ}\text{C} + 50\,^{\circ}\text{C GPa}^{-1} \times P$. This means that the increment or decrement with P in T_g strongly depends on the chemical composition of substances.

3.2. Structural properties of amorphous TiO_2

It was found that amorphous TiO_2 models at the density of 3.80 g cm^{-3} have a slightly octahedral network structure with the mean coordination number $Z_{Ti-O} \approx 6.0$ and $Z_{O-Ti} \approx 3.0$ [23]. It is interesting to see the structure of amorphous TiO_2 models at other ambient pressure densities such as 4.00 and 4.20 g cm^{-3}. As shown in figure 3, the PRDFs of the TiO_2 models change slightly with increasing density from 3.80 to 4.20 g cm^{-3}, indicating the similar structure of the models. Two important remarks can be made here. First, a splitting of the first peak in the PRDF for the Ti–Ti pair has been found for all densities studied, like that observed in experiment, i.e. the prepeak is centered at around 3.00 Å and the main peak is at 3.47 Å, versus 3.00 Å and 3.55 Å obtained in experiment, respectively [9] (see table 2). As discussed in [9], the shorter Ti–Ti interatomic distance of 3.00 Å is related to the pairs of Ti atoms centering octahedra linked by the edge, and the longer distance of 3.55 Å is of the pairs of Ti atoms from octahedra having a common vertex. The same explanation can be drawn here for our systems. However, the prepeak becomes less pronounced at higher density, indicating slight changes in the fraction of octahedra linked by the edge in our models. Second, a small peak at around 3.70 Å for the PRDF of the O–O pair has been found for all three models. Accordance to our recent calculations [23], such a small peak occurs only at relatively low temperatures together with the appearance of the prepeak in the PRDF for the Ti–Ti pair

Table 2. Structural characteristics of amorphous TiO_2. r_{ij}: position of the first peaks in PRDFs; g_{ij}: the height of the first peaks in the PRDFs; Z_{ij}: the average coordination number (1–1 for the Ti–Ti pair, 1–2 for the Ti–O pair, 2–1 for the O–Ti pair, 2–2 for the O–O pair).

Density		r_{ij} (Å)			g_{ij}			Z_{ij}			
(g cm^{-3})	References	1–1	1–2	2–2	1–1	1–2	2–2	1–1	1–2	2–1	2–2
3.80	[23]	3.00–3.47	1.85	2.59	3.15	8.27	2.75	8.92	5.76	2.88	10.7
4.00	Present work	3.02–3.45	1.85	2.56	3.22	7.91	2.78	9.38	5.88	2.94	11.2
4.20	Present work	3.02–3.41	1.85	2.52	3.04	7.93	2.95	9.92	6.03	3.02	11.6
	Exp. data [9]	3.00–3.55	1.96	2.67	4.47	5.60	2.97	8.80	5.40	2.70	10.5

Table 3. Fraction of Ti atoms with coordination number $Z_{Ti-O} = 4$, 5, 6, 7 and 8; and fraction of O atoms with $Z_{O-Ti} = 2$, 3 and 4 in amorphous TiO_2.

Density	Z_{Ti-O}					Z_{O-Ti}		
(g cm^{-3})	4	5	6	7	8	2	3	4
3.80	0.007	0.264	0.689	0.038	0.002	0.162	0.793	0.045
4.00	0.000	0.183	0.754	0.063	0.000	0.111	0.839	0.050
4.20	0.000	0.113	0.747	0.135	0.005	0.078	0.829	0.093

and it is related to the typical O–O distance of octahedra linked by the edge. Therefore, the appearance of an additional small peak in PRDF for the O–O pair at low temperatures is related to a greater degree of close-packing structure in the system, i.e. it is related to the occurrence of an octahedral phase in the system. Such a small peak at around 3.70 Å in the PRDF for the O–O pair was also found experimentally for TiO_2 layers obtained by sol–gel dip coating [9].

More details of the structure of the models can be found in tables 2 and 3. One can see that the mean interatomic distance for Ti–Ti and O–O pairs becomes shorter while the mean coordination number for all atomic pairs increases with increasing density of the system, indicating the formation of a greater degree of close-packing structure (table 2). However, the changes are not very great, in that the structure of the models at the three densities remains a slightly distorted octahedral network. The octahedrality is enhanced with increasing density. We also show the coordination number and bond-angle distributions for the model at 4.00 g cm^{-3}; they are very similar to those observed previously for the model at 3.80 g cm^{-3} [23] in that the Ti atoms are mainly surrounded by six O ones and the O atoms are surrounded by three Ti (see figures 4 and 5). The Ti–O–Ti bond-angle distribution also has two peaks related to the two types of linkage between octahedra in the system.

Moreover, although we found that amorphous TiO_2 has an octahedral network structure with mean $Z_{Ti-O} \approx 6$ and $Z_{O-Ti} \approx 3$ at all three different densities studied, i.e. it is locally similar to the local structure of crystalline TiO_2 in which it was found that $Z_{Ti-O} = 6$ and $Z_{O-Ti} = 3$ [9], the former differs from the latter by interatomic distances that vary over a wide range and by the existence of a significant number of structural defects (i.e. Ti atoms with $Z_{Ti-O} \neq 6$ and O atoms with $Z_{O-Ti} \neq 3$; see table 3). On the other hand, table 3 shows that the fraction of Ti atoms with $Z_{Ti-O} = 6$ and the fraction of O atoms with $Z_{O-Ti} = 3$ dominate in the system at three different densities and it reaches a maximum value at the density of 4.00 g cm^{-3}, while the fraction of relatively under-coordinated atoms (Ti and O) decreases with increasing density. In contrast, the fraction of over-coordinated atoms increases (see table 3). Such under-coordinated or over-coordinated Ti and O atoms can be considered as structural

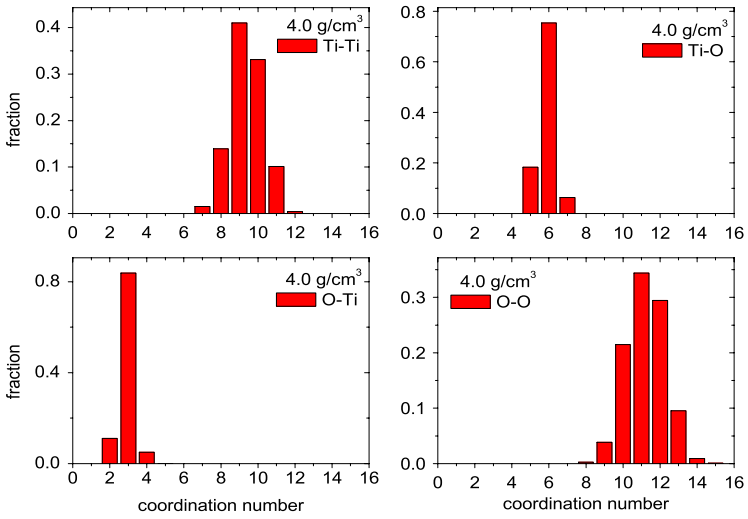

Figure 4. Coordination number distributions of the amorphous TiO_2 model at 4.00 g cm^{-3} and at $T = 350$ K.

(This figure is in colour only in the electronic version)

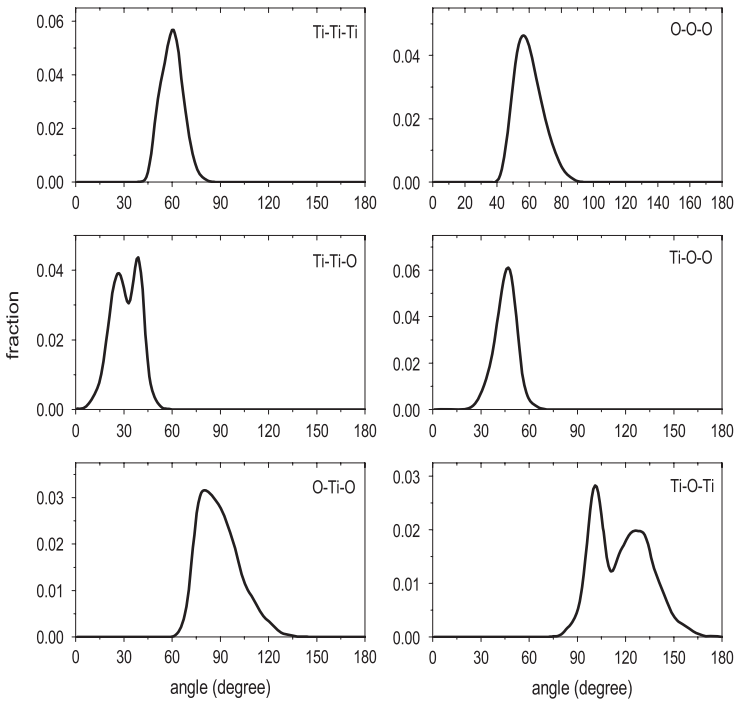

Figure 5. Bond-angle distributions of the amorphous TiO_2 model at 4.00 g cm^{-3} and at $T = 350$ K.

point defects in amorphous TiO_2. The differences between fractions of structural defects in the amorphous TiO_2 models at three different densities are significant. In addition, due to the structure lacking periodic order, there is a possible large amount of another type of point

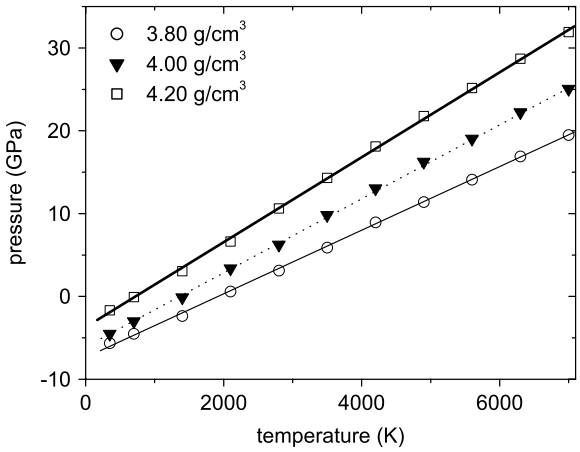

Figure 6. Temperature dependence of the system pressure along the isochore for liquid and amorphous TiO_2 at three different densities.

Table 4. Parameters of the equation $P = aT + b$ (GPa) for the isochore of the TiO_2 models.

Density (g cm^{-3})	a (10^{-4} GPa K^{-1})	b (GPa)
3.80	38.300 ± 0.316	-7.350 ± 0.131
4.00	45.001 ± 0.317	-6.145 ± 0.131
4.20	51.502 ± 0.391	-3.761 ± 0.162

defect in amorphous TiO_2, i.e. vacancy-like defects [34]. It was found that there is a significant amount of large pores, which can exchange their position with the nearest-neighbor atoms and act as vacancies in the diffusion process in amorphous Al_2O_3 [34]. For crystalline TiO_2, it was pointed out that point defects can play a major role in a variety of surface phenomena, i.e. in bulk-assisted reoxidation, in restructuring and reconstruction processes or in the adsorption of sulfur and other inorganic compounds (see [12] and references therein). Similar phenomena for an amorphous TiO_2, probably, can be expected especially for thin films or for nanoparticles in which the surface plays an important role in the structure and properties of substances.

It is also of interest to show the temperature dependence of pressure in the system along the isochore at three different densities, and that it can be described well for temperatures in the range from 350 to 7000 K by the following equation of state: $P = aT + b$ (GPa) (see figure 6). Parameters for the equation are given in table 4.

3.3. Temperature dependence of the diffusion constant in liquid TiO_2

We study diffusion only in the liquid TiO_2 at 3.80 g cm^{-3}, and due to close structures, similar results for diffusion in the models at 4.00 and 4.20 g cm^{-3} can be expected. One can find the diffusion constant of atomic species in the system via the Einstein relation: $\lim_{t\to\infty} \frac{\langle r^2(t)\rangle}{6t} = D$; here $\langle r^2(t)\rangle$ is the mean-squared displacement (MSD) of atoms. The time dependence of $\langle r^2(t)\rangle$ for Ti atoms in liquid TiO_2 at three different temperatures can be found in figure 7. One can see clearly two regimes in the curves: a ballistic one at short times and a diffusive one at longer times. At low temperatures, these two regimes are separated by a plateau regime. The plateau regime is related to the caging effects, which are more pronounced at lower temperatures. Similar results have been obtained for O atoms (not shown).

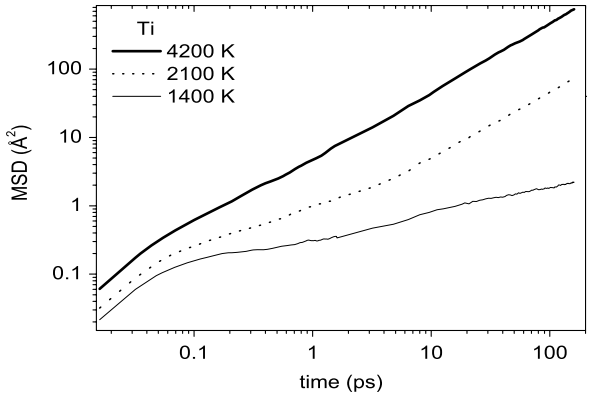

Figure 7. Mean-squared displacement of Ti atoms in liquid 3.80 g cm^{-3} TiO_2 models at three different temperatures.

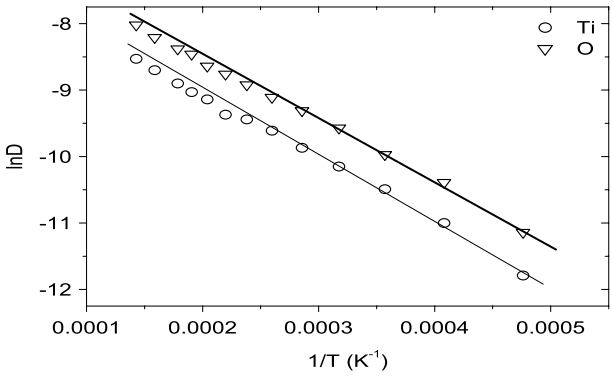

Figure 8. $1/T$ dependence of the diffusion constant of atoms in liquid 3.80 g cm^{-3} TiO_2 models. The straight lines serve as a guide for the eyes.

The temperature dependence of the diffusion constant of atomic species in liquid TiO_2 has been found, and it is presented in figure 8; the error of estimating the diffusion constant is smaller than the size of the symbol presented in the curves. One can see that at relatively low temperatures above the melting point it follows an Arrhenius law and it deviates from an Arrhenius law at higher temperatures. However, the deviation is not strong, unlike those observed for other network structure liquid oxides such as SiO_2, Al_2O_3 and GeO_2 [40–43]. With regard to an Arrhenius law, $D = D_0 \exp(-\frac{E}{k_B T})$, we found that the pre-exponential constant D_0 is equal to 9.045×10^{-4} and 13.085×10^{-4} cm^2 s^{-1} for Ti and O, respectively. However, the activation energy is rather small: 0.855 and 0.805 eV for Ti and O, respectively. We have no experimental data for liquid TiO_2 to compare with. However, such a value for an activation energy is much smaller than that observed in practice for silica, where it is equal to 4.70 and 6.00 eV for oxygen and silicon, respectively [44, 45]. Low activation energy for diffusion of atomic species in liquid TiO_2 might be related to the different contributions of ionic and covalent bonds to the cohesive energy of the system compared with those that exist in silica (i.e. it is worth noticing that TiO_2 is an iono-covalent system).

Table 5. Density dependence of the structural characteristics of liquid TiO_2 upon pressurization at constant $T = 2800$ K.

		r_{ij}			Z_{ij}			
ρ (g cm^{-3})	Pressure (GPa)	Ti–Ti	Ti–O	O–O	Ti–Ti	Ti–O	O–Ti	O–O
3.8	2.92	3.25	1.81	2.52	8.54	5.52	2.76	10.51
4.1	8.33	3.29	1.81	2.48	9.31	5.79	2.89	11.15
4.4	15.70	3.23	1.81	2.44	10.18	6.11	3.06	11.79
4.7	25.80	3.16	1.81	2.40	10.91	6.49	3.25	12.21
5.0	39.83	3.10	1.81	2.35	11.45	6.86	3.43	12.69
5.3	56.93	3.04	1.81	2.32	11.98	7.22	3.61	13.13

3.4. Liquid–liquid phase transition in liquid TiO_2

For crystalline TiO_2, under a high pressure of 20 GPa and at 770 °C, a pressure-induced rutile to baddeleyite transition has been found experimentally. It is accompanied with a volume reduction of about 9%, and the coordination number of Ti increases from six to seven [46]. High-pressure crystalline TiO_2 has the same structure as baddeleyite, the stable phase of ZrO_2 at ambient conditions [46]. On the other hand, the pressure-induced ldl → hdl phase transition has been found in different tetrahedral network structure liquids such as SiO_2, H_2O, GeO_2 or $Al_2O_3{\cdot}2SiO_2$ (see [47–51] and references therein). And such a transition is often accompanied with an anomalous diffusion of atomic species, wherein the diffusivity first increases and then decreases with pressure. Therefore, it is of interest to carry out a study on the pressure-induced ldl → hdl phase transition in liquid TiO_2, since it has not been studied yet.

The initial 3.8 g cm^{-3} model of liquid TiO_2 was isotropically compressed at constant $T = 2800$ K by steps of 0.3 up to 5.3 g cm^{-3}, when the ldl → hdl transition in liquid TiO_2 completely occurs. After each volume change the system was relaxed over 10^4 MD steps to reach an equilibrium state at constant density and temperature. In order to calculate the diffusion constant of the atomic species in equilibrium liquids at each density, the system was relaxed further for 10^5 MD steps. One can see in table 5 that the mean interatomic distance for Ti–Ti and O–O pairs decreases with growing density of the system (or pressure) while the mean coordination number for all atomic pairs increases, indicating the formation of a greater degree of close-packing structure caused by pressurization. In contrast, the mean interatomic distance for the Ti–O pair remains unchanged with density due to the strong Ti–O bond. Moreover, at the ambient pressure density of around 3.8–4.1 g cm^{-3}, liquid TiO_2 (i.e. the ldl form) has an octahedral network structure with $Z_{\mathrm{Ti-O}} \approx 6$ and $Z_{\mathrm{O-Ti}} \approx 3$, and at 5.0–5.3 g cm^{-3} we found the new hdl form with $Z_{\mathrm{Ti-O}} \approx 7$ and $Z_{\mathrm{O-Ti}} \approx 3.5$. This confirms our suggestion above that the ldl → hdl transition may occur at around 5.0 g cm^{-3}, and it leads to the deviation from linearity of the density dependence of T_g of the liquid TiO_2 models (see figure 2). This means that we clearly found an ldl → hdl transition in the liquid TiO_2 models (see table 5). More details of the structure evolution upon the ldl → hdl transition in liquid TiO_2 models can be found via the density dependence of TiO_n units in figure 9. While the fraction of TiO_4 and TiO_5 decreases with increasing density, the fraction of TiO_7 and TiO_8 increases. At around 5.0–5.3 g cm^{-3}, TiO_7 units dominate in the system, ensuring that the ldl → hdl transition occurs completely. In contrast, the fraction of TiO_6 increases, passes through a maximum at around the density of 4.3 g cm^{-3} and then it decreases with further increasing density of the system (figure 9). Figure 9 also shows that the structure evolution in liquid TiO_2 caused by pressurization is gradual, unlike those observed in crystalline TiO_2 [46]. On the other hand, in the high-pressure crystalline form, the Ti atoms are equally surrounded by seven O atoms with $Z_{\mathrm{Ti-O}} = 7$ [46];

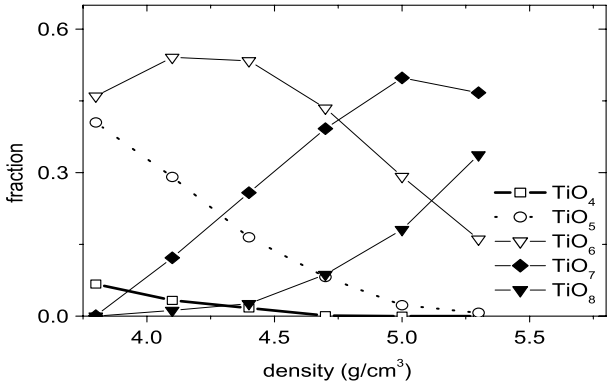

Figure 9. Density dependence of structural TiO_n units in liquid TiO_2 at 2800 K under compression.

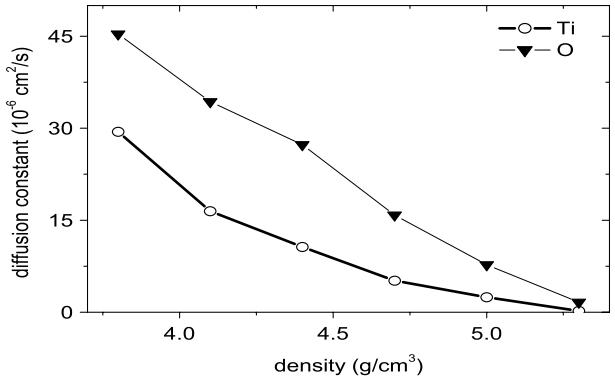

Figure 10. Density dependence of the diffusion constant of atomic species in liquid TiO_2 at 2800 K under compression.

the hdl form differs from the high-pressure crystalline form by interatomic distances varying over wide value range and by the existence of a significant number of structural point defects (i.e. TiO_5, TiO_6 and TiO_8). It is essential to notice that the percentage of TiO_7 in the hdl form of the liquid TiO_2 model at 2800 K is just equal to 50%, and the percentage for defects is also equal to 50%.

It is interesting to study the density dependence of diffusivity of atomic species in liquid TiO_2 upon pressurization; it monotonically decreases with increasing density (figure 10). The error in estimating the diffusion constant is smaller than the size of the symbol presented in the curves. This means that the ldl $\rightarrow$ hdl transition in liquid TiO_2 models is not accompanied by an anomalous diffusion, i.e. the diffusivity first increases and then decreases with pressure, unlike those observed in tetrahedral network structure liquids. The important role of the intermediate structural units such as TO_5 (T $=$ Si, Ge, Al etc) has been pointed out for an anomalous diffusion to occur during the ldl $\rightarrow$ hdl transition from a tetrahedral to an octahedral network structure in several liquids (i.e. transformation from the form with $Z_{T-O} = 4$ to the one with $Z_{T-O} = 6$). It was found that the maximum diffusivity occurs when TO_5 units are the most abundant in the systems [51]. In the present work, due to the lack of intermediate structural units for the ldl $\rightarrow$ hdl transition in liquid TiO_2 (i.e. it just transforms from the form

with $Z_{\mathrm{Ti-O}} = 6$ to the one with $Z_{\mathrm{Ti-O}} = 7$) the anomalous diffusion of atomic species does not occur.

4. Conclusions

Our calculations show that in the density range from 3.80 to 4.20 g cm^{-3}, i.e. the ambient pressure density of crystalline and amorphous TiO_2, amorphous TiO_2 has a slightly distorted octahedral network structure with the mean coordination number $Z_{\mathrm{Ti-O}} \approx 6.0$ and $Z_{\mathrm{O-Ti}} \approx 3.0$. This is in good agreement with the experimental data. The glass transition temperature of liquid TiO_2 at ambient pressure is at around 1200 K. Moreover, we found a linear density dependence of T_g for liquid TiO_2: $T_g = a + b\rho$. Here, $a = 352$ K, $b = 235.43$ cm^3 g^{-1} and ρ is the density of liquid TiO_2 in g cm^{-3}. However, at high density, strong deviation from linearity (i.e. from $T_g = a + b\rho$) has been found. The phenomenon is related to the structural transformation from a low-density form to a high-density form of liquid TiO_2. Furthermore, we found that the temperature dependence of the diffusion constant in 3.80 g cm^{-3} liquid TiO_2 follows an Arrhenius law at relatively low temperatures and it deviates from it at higher ones, like those observed in other network structure oxides. We found an ldl $\rightarrow$ hdl transition in liquid TiO_2, and it is not accompanied by an anomalous diffusion of atomic species. Due to the limited number of works related to the simulation of liquid and amorphous TiO_2, our results give an additional understanding of such an important material.

Acknowledgments

The author is grateful for financial support from the Japan Society for the Promotion of Science via a JSPS Invitation Research Fellowship. The author also thanks Professor T Odagaki for hospitality during his stay at Kyushu University.

References

[1] Jamieson J C and Olinger B 1968 *Science* **161** 893
[2] Kruczynski L, Gesser H D, Turner C W and Speer E A 1981 *Nature* **291** 399
[3] Matsui M and Akaogi M 1991 *Mol. Simul.* **6** 239
[4] Leinen D, Fernandez A, Espinos J P, Caballero A, Justo A and Gonzalez-Elipe A R 1994 *Thin Solid Films* **241** 175
[5] Pouilleau J, Devilliers D, Garrido F, Durand-Vidal S and Mahe E 1997 *Mater. Sci. Eng.* B **47** 235
[6] Amor S B, Baud G, Besse J P and Jacquet M 1997 *Mater. Sci. Eng.* B **47** 110
[7] Ayers M R and Hunt A J 1998 *Mater. Lett.* **34** 290
[8] Bach U, Lupo D, Comte P, Moser J E, Weissortel F, Salbeck J, Spreitzer H and Gratzel M 1998 *Nature* **395** 583
[9] Petkov V, Holzhuter G, Troge U, Gerber Th and Himmel B 1998 *J. Non-Cryst. Solids* **231** 17
[10] Amor S G, Guedri L, Baud G, Jacquet M and Ghedira M 2002 *Mater. Chem. Phys.* **77** 903
[11] Tsyganov I, Maitz M F, Wieser E, Prokert F, Richter E and Rogozin A 2003 *Surf. Coat. Technol.* **174/175** 591
[12] Diebold U 2003 *Surf. Sci. Rep.* **48** 53
[13] Kiema G K, Colgan M J and Brett M J 2005 *Sol. Energy Mater. Sol. Cells* **85** 321
[14] Modes T, Scheffel B, Metzner Chr, Zywitzki O and Reinhold E 2005 *Surf. Coat. Technol.* **200** 306
[15] Pathan H M, Min S-K, Desai J D, Jung K-D and Joo O-S 2006 *Mater. Chem. Phys.* **97** 5
[16] Padmanabhan K, Harvey N E, Kurel P, Talagala P, Naik R, Auner G W, Naik V M, Suryanarayanan R, Thevuthasan S and Shutthanandan V 2006 *Nucl. Instrum Methods Phys. Res.* B **249** 540
[17] Kleiman A, Marquez A and Lamas D G 2007 *Surf. Coat. Technol.* **201** 6358
[18] Weinberg B and Garber R 1995 *Appl. Phys. Lett.* **66** 2409
[19] Exarbos G and Hess N 1992 *Thin Solid Films* **220** 254
[20] Lottici P, Bersani D, Bragnini M and Montenero A 1993 *J. Mater. Sci.* **28** 177
[21] Spitzer A, Reisinger H, Willer J, Honlein W, Cerva H and Zorn G 1991 *Proc. INFOS91 (Liverpool)* p 187

[22] Arsov L, Kormann C and Plieth W 1991 *J. Raman. Spectrosc.* **22** 573
[23] Hoang V V 2007 *Phys. Status Solidi* b **244** 1280
[24] Kim D W, Enomoto N, Nakagawa Z and Kawamura K 1996 *J. Am. Ceram. Soc.* **79** 1095
[25] Catlow C R A, Freeman C M and Royal R L 1985 *Physica* B **131** 1
[26] Catlow C R A and James R 1982 *Proc. R. Soc.* A **384** 157
[27] Sawatari H, Iguchi E and Tilley R J D 1982 *J. Phys. Chem. Solids* **43** 1147
[28] Mostoller M and Wang J C 1985 *Phys. Rev.* B **32** 6773
[29] Post J E and Burnham C W 1986 *Am. Mineral.* **71** 142
[30] Roux H I and Glasser L J 1997 *J. Mater. Chem.* **7** 843
[31] Swamy V and Gale J D 2000 *Phys. Rev.* B **62** 5406
[32] Oliver P M, Watson G W, Kelsey E T and Parker S C 1997 *J. Mater. Chem.* **7** 563
[33] Collins D R and Smith W 1996 *Council for the Central Laboratory of Research Councils, Daresbury Research Report* DL-TR-96-001
[34] Hoang V V 2004 *Phys. Rev.* B **70** 134204
[35] Mergel D, Buschendorf D, Eggert S, Grammes R and Samset B 2000 *Thin Solid Films* **371** 218
[36] Micoulaut M, Guissani Y and Guillot B 2006 *Phys. Rev.* E **73** 031504
[37] Lide D R (ed) 1996 *CRC Handbook of Chemistry and Physics* (New York: CRC Press)
[38] Swamy V, Kuznetsov A, Dubrovinsky L S, McMillan P F, Prakapenka V B, Shen G and Muddle B C 2006 *Phys. Rev. Lett.* **96** 135702
[39] Bagdassarov N S, Maumus J, Poe B, Slutskiy A B and Bulatov V K 2004 *J. Phys. Chem. Glasses* **45** 197
[40] Horbach J and Kob W 1999 *Phys. Rev.* B **60** 3169
[41] Hoang V V 2006 *New Developments in Condensed Matter Physics* (New York: Nova Science)
[42] Hoang V V, Zung H and Hai N T 2007 *J. Phys.: Condens. Matter* **19** 116104
[43] Hoang V V, Tuan Anh N H and Zung H 2007 *Physica* B **394** 39
[44] Brebec G, Seguin R, Sella C, Bevenot J and Martin J C 1980 *Acta Metall.* **28** 327
[45] Mikkelsen J C 1984 *Appl. Phys. Lett.* **45** 1187
[46] Sato H, Endo S, Sugiyama M, Kikegawa T, Shimomura O and Kusaba K 1991 *Science* **251** 786
[47] Errington J R and Debenedetti P G 2001 *Nature* **409** 318
[48] Shell M S, Debenedetti P G and Panagiotopoulos A Z 2002 *Phys. Rev.* E **66** 011202
[49] Hoang V V, Tuan Anh N H and Zung H 2007 *Physica* B **390** 17
[50] Hoang V V, Hung N H and Linh N N 2006 *Phys. Scr.* **74** 697
[51] Hoang V V 2007 *Phys. Lett.* A **368** 499